Fission yeast Alp14 is a dose-dependent plus end–tracking microtubule polymerase

Jawdat Al-Bassam[a,b,*], Hwajin Kim[c,*], Ignacio Flor-Parra[c], Neeraj Lal[a], Hamida Velji[b], and Fred Chang[c]

[a]Department of Molecular and Cellular Biology, University of California, Davis, Davis, CA 95616; [b]Department of Biological Chemistry and Molecular Pharmacology, Harvard Medical School, Boston, MA 02115; [c]Department of Microbiology and Immunology, Columbia University College of Physicians and Surgeons, New York, NY 10032

ABSTRACT **XMAP215/Dis1 proteins are conserved tubulin-binding TOG-domain proteins that regulate microtubule (MT) plus-end dynamics. Here we show that Alp14, a XMAP215 orthologue in fission yeast, *Schizosaccharomyces pombe*, has properties of a MT polymerase. In vivo, Alp14 localizes to growing MT plus ends in a manner independent of Mal3 (EB1). *alp14*-null mutants display short interphase MTs with twofold slower assembly rate and frequent pauses. Alp14 is a homodimer that binds a single tubulin dimer. In vitro, purified Alp14 molecules track growing MT plus ends and accelerate MT assembly threefold. TOG-domain mutants demonstrate that tubulin binding is critical for function and plus end localization. Overexpression of Alp14 or only its TOG domains causes complete MT loss in vivo, and high Alp14 concentration inhibits MT assembly in vitro. These inhibitory effects may arise from Alp14 sequestration of tubulin and effects on the MT. Our studies suggest that Alp14 regulates the polymerization state of tubulin by cycling between a tubulin dimer–bound cytoplasmic state and a MT polymerase state that promotes rapid MT assembly.**

Monitoring Editor
Kerry S. Bloom
University of North Carolina

Received: Mar 13, 2012
Revised: Jun 5, 2012
Accepted: Jun 8, 2012

INTRODUCTION

Microtubules (MTs) are dynamic polymers of αβ-tubulin dimers that play diverse functions in processes such as cell division, intracellular transport, and cellular morphogenesis. Many of the dynamic behaviors of MTs are regulated by proteins at the MT plus end (Akhmanova and Steinmetz, 2008). Although many such proteins have now been identified, in most cases, little is known about how these proteins regulate the MT at a mechanistic level. The conserved XMAP215/Dis1 family of proteins is emerging as key regulators of MT assembly. XMAP215 was initially identified as an activity that promotes the formation of long MTs in *Xenopus* extracts (Gard and Kirschner, 1987). Genetic and cell biological studies implicate this protein family as critical regulators of MT assembly in cell types ranging from yeasts and plants to humans (Gard *et al.*, 2004; Al-Bassam and Chang, 2011). Loss of function of XMAP215/Dis1 orthologues generally leads to defective monopolar or short mitotic spindles and to short interphase MTs that grow slowly. Many proteins in this family localize to MT plus ends and to sites such as kinetochores and centrosomes and play essential roles in regulating MT dynamics for chromosome segregation. In vitro studies suggest that the recombinant XMAP215 (*Xenopus* orthologue) is a processive MT polymerase that accelerates the rate of MT assembly while bound at the growing MT plus ends (Brouhard *et al.*, 2008). XMAP215 proteins also have inhibitory effects on MTs under in vitro conditions where soluble tubulin is absent, although the in vivo relevance of this activity remains to be established (Shirasu-Hiza *et al.*, 2003; van Breugel *et al.*, 2003; Brouhard *et al.*, 2008). Important questions remain about the molecular mechanisms of how the XMAP215/Dis1 family localize to growing MT plus ends and function to promote MT assembly.

A key feature of XMAP215/Dis1 family is their ability to bind to soluble αβ-tubulin dimers through conserved tumor overexpressed

This article was published online ahead of print in MBoC in Press (http://www.molbiolcell.org/cgi/doi/10.1091/mbc.E12-03-0205) on June 13, 2012.

*These authors contributed equally to this work.

Address correspondence to: Fred Chang (fc99@columbia.edu), Jawdat Al-Bassam (jawdat@ucdavis.edu).

Abbreviations used: MT, microtubule; +TIP, microtubule plus end protein; TOG, tumor overexpressed gene.

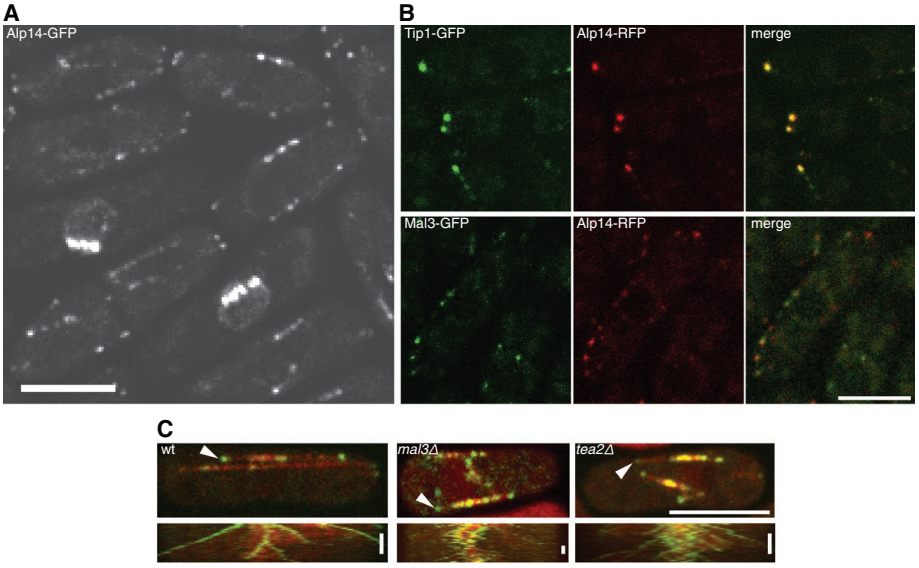

FIGURE 1: Alp14 tracks MT plus ends in *S. pombe* cells. (A) Images of fission yeast cells expressing Alp14-GFP fusion protein (FC1907). Alp14 is seen as cytoplasmic dots aligned in linear tracks in interphase cells. In mitotic cells, it is present in bright dots on the mitotic spindle. (B) Alp14 colocalization with other +TIP proteins. Images of cells (FC2347, FC2336) coexpressing Alp14-RFP with Mal3-GFP (EB1) or Tip1-GFP (CLIP-170). (C) Images of cells expressing Alp14-GFP and mRFP-Atb2 (tubulin) in wild-type (FC2493), *tea2*Δ (FC2471), and *mal3*Δ (FC2472) backgrounds. Kymographs were derived from images of MT bundles marked by arrowheads. Streaks of Alp14-GFP show plus end tracking of Alp14-GFP in these strains. Scale bar, 5 μm. Timescale bar, 60 s.

gene (TOG) domains at their N-termini (Al-Bassam *et al.*, 2007; Al-Bassam and Chang, 2011; Slep and Vale, 2007). TOG domains form paddle-like structures composed of helical HEAT repeats and bind to a αβ-tubulin heterodimer in solution using conserved intra-HEAT repeat loops (Al-Bassam *et al.*, 2007). The budding yeast orthologue Stu2p is a homodimer that contains two sets of two TOG domains, whereas mammalian and fly orthologues are monomers and contain five TOG domains. Stu2 (dimer) and XMAP215 (monomer) bind a single tubulin dimer, and electron microscopy studies suggest that the TOG domains wrap around a tubulin dimer to form a globular complex (Al-Bassam *et al.*, 2006; Brouhard *et al.*, 2008). TOG domains are critical for XMAP215 MT polymerase activity (Al-Bassam *et al.*, 2006; Brouhard *et al.*, 2008; Currie *et al.*, 2011). Point mutations inactivating XMAP215 TOG domains suggest that a decrease in the affinity of molecules for tubulin dimer correlate with a decrease in the ability to promote MT assembly in vitro (Widlund *et al.*, 2011). How these TOG domains function in MT polymerase and plus end tracking activities, however, is still poorly understood. It is debated, for instance, whether TOG domains bind to tubulins in the MT lattice or only to soluble tubulin dimers, and whether TOG domains target these proteins for MT plus end tracking. The in vivo relevance of the in vitro observations of XMAP215 to other family members remains to be established.

The fission yeast *Schizosaccharomyces pombe* is a genetically tractable model organism useful for studying conserved aspects of MT regulation (Sawin and Tran, 2006; Bratman and Chang, 2008). Interphase MTs are organized in three to five bundles oriented along the long axis of these rod-shaped cells. The relatively small number of MTs makes it possible to track and quantitatively measure the dynamics of the MT plus ends in vivo. *S. pombe* contains two XMAP215/Dis1 orthologues: Dis1 and Alp14. Null mutants of each single gene are viable, but the double mutant is lethal (Garcia *et al.*, 2001). Previous studies on these genes focused largely on their mitotic functions, especially at the kinetochore (Nabeshima *et al.*, 1995; Garcia *et al.*, 2001; Hsu and Toda, 2011). Alp14 interacts with Alp7, an orthologue of transforming acidic coiled-coil proteins, and its nuclear localization is cell cycle regulated by the Ran GTPase system (Sato *et al.*, 2004; Sato and Toda, 2007). A recent study suggests that not all proteins in this family act the same: Dis1 localizes to regions of MT bundling in the spindle midzone and interphase arrays and may contribute to MT bundling and not to interphase MT dynamics (Roque *et al.*, 2010).

Here we study the molecular activities of *S. pombe* Alp14 using in vivo and in vitro approaches. In vivo, Alp14 localizes to growing MT plus ends, and null mutants of *alp14* exhibit short MTs with decreased MT assembly rates and frequent MT pauses. In vitro total internal reflection fluorescence (TIRF) microscopy studies show that recombinant Alp14 tracks MT plus ends and accelerate assembly by twofold to threefold. Mutational analyses show that the N-terminal TOG domains, which bind to tubulin dimer, and the C-terminal region, which binds to the MT lattice, all contribute to MT plus end localization and polymerase activity. In the course of our studies, we discovered that Alp14 activities are highly dose dependent both in vivo and in vitro. Mild (threefold) overexpression of Alp14 or even of just its TOG domains causes dramatic MT loss in vivo, whereas increasing Alp14 concentration in vitro decreases efficiency of its MT assembly activity. Our findings suggest that the balance between Alp14 and free tubulin concentrations is critical for regulation of MT assembly.

RESULTS

Alp14 tracks MT plus ends in vivo independently of other plus end–tracking proteins.

We examined Alp14 localization in living fission yeast cells using a functional Alp14–green fluorescent protein (GFP) fusion that is expressed at near endogenous levels from the *alp14* chromosomal locus (Sato *et al.*, 2004). During mitosis, Alp14-GFP localized to multiple dots on the mitotic spindle and spindle pole bodies, as seen previously (Nakaseko *et al.*, 2001; Sato *et al.*, 2004; Figure 1A). In interphase cells, Alp14-GFP localized to cytoplasmic dots. These moved in a linear manner, mostly from the cell center toward the cell tips (see also Nakaseko *et al.*, 2001; Sato *et al.*, 2004). Dual imaging of Alp14-GFP with red fluorescent protein (RFP)–labeled tubulin (Snaith *et al.*, 2010) confirmed that these Alp14 dots track with growing MT plus ends (Figure 1C and Supplemental Movie S1). Alp14 was also sometimes detected at a very low level on the MT lattice. We did not detect any Alp14 accumulation on the plus ends of shrinking MTs. Multiple Alp14 dots within each MT bundle may represent MT plus ends growing within each MT bundle. Alp14-GFP dots largely colocalized with other MT plus end–tracking proteins (termed +TIPs) Mal3 (EB1) or Tip1 (CLIP-170; Figure 1B; Beinhauer *et al.*, 1997; Busch and Brunner, 2004).

Next we tested whether Alp14 localization at growing MT plus ends is dependent on other +TIP proteins. EB proteins are believed

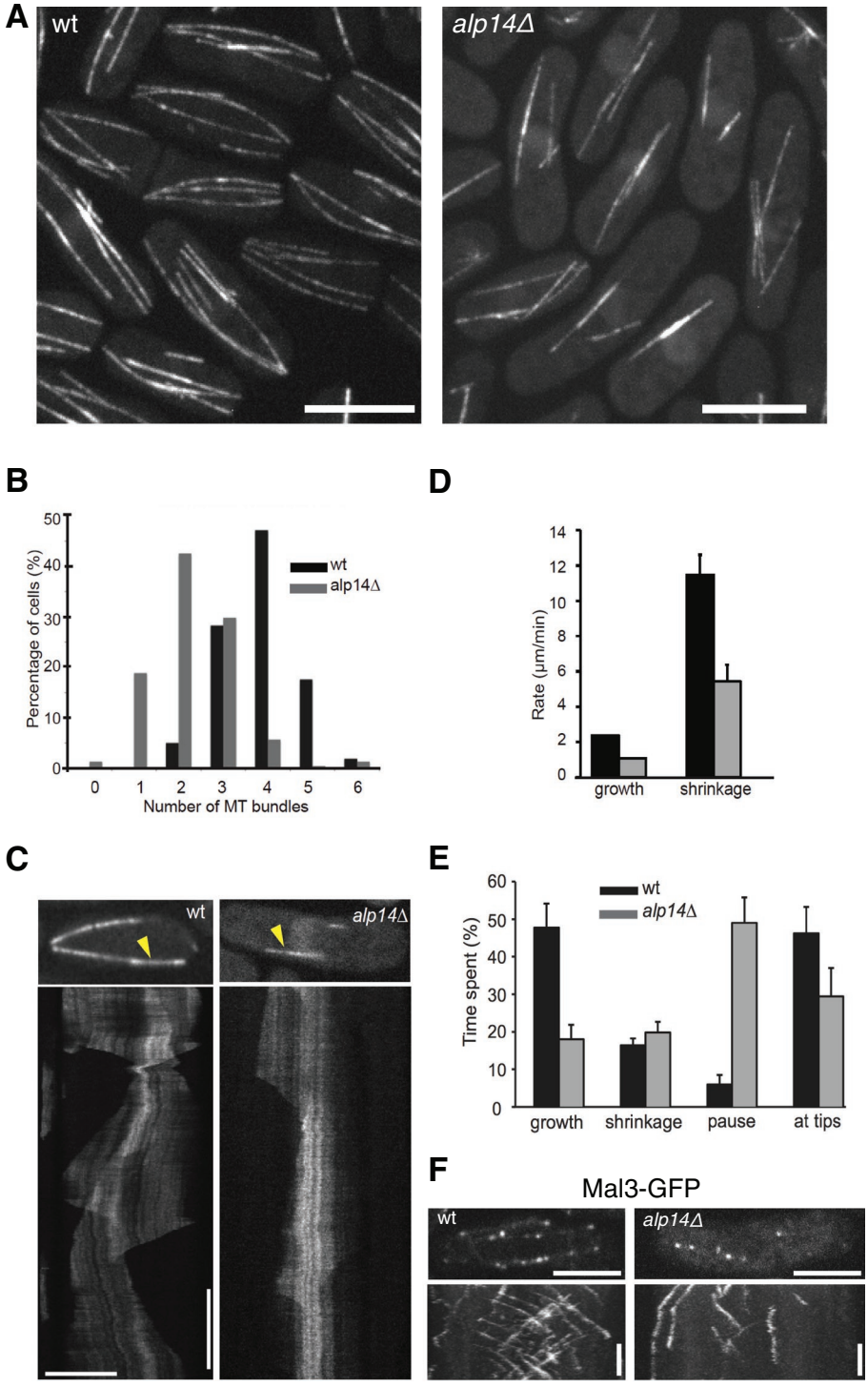

FIGURE 2: *alp14*-null mutant cells display impaired microtubule assembly. (A) Wild-type and *alp14*Δ mutant cells expressing GFP-tubulin (FC1234, FC2332). Note the decreased number of MT bundles in *alp14*Δ cells compared with wild-type cells. Scale bar, 5 μm. (B) Histogram of number of interphase MT bundles in interphase cells in wild-type ($n = 159$) and *alp14*Δ ($n = 228$) cells. (C) Kymographs derived from time-lapse images of a MT bundle in wild-type and *alp14*Δ cells expressing GFP-tubulin. Scale bar, 5 μm. Timescale bar, 30 s. (D) Dynamics of individual MT plus ends. Rates of MT assembly and disassembly in wild-type ($n = 38$) and *alp14*Δ ($n = 40$) cells. (E) Percentage of time spent in each MT dynamic phase. Pause was defined as <0.5 mm/min change. Note that these measurements do not account for very small, transient changes seen in the ragged patterns in the *alp14*Δ kymographs. Twenty-two microtubules were measured in 18 wild-type cells. Twenty-six microtubules were measured in 23 *alp14*Δ cells. (F) Images and kymographs of cells expressing Mal3-GFP as a marker of plus end dynamics in wild-type and *alp14*Δ background (FC1439, FC2328). Scale bar, 5 μm. Timescale bar, 30 s.

to recruit many +TIPs to MT plus ends, including the Msps (*Drosophila* XMAP215 orthologue; Honnappa *et al.*, 2009; Akhmanova and Steinmetz, 2011; Currie *et al.*, 2011). In *S. pombe*, Mal3 (EB1) may load the kinesin Tea2 onto the MT, which in turn transports Tip1 (CLIP-170) to the MT plus end (Busch *et al.*, 2004; Bieling *et al.*, 2007). We found that Alp14-GFP still localized at MT plus ends in *mal3*Δ (EB1) and *tea2*Δ (kinesin) mutant cells, even though the MTs themselves were abnormally short (Figure 1C and Supplemental Movie S2). Thus Alp14 may not be strictly dependent on these other +TIPs for MT plus end tracking.

*alp14*Δ mutants exhibit decreased MT assembly rate and increased frequency of pauses

To test the role of Alp14 on MT dynamics in vivo, we characterized *alp14*Δ-null mutant cells. As shown previously, these cells were viable but grew slowly and formed abnormally bent cell morphologies, similar to other mutants with defective MTs (Figure 2A; Nakaseko *et al.*, 2001; Sawin and Tran, 2006). To observe the dynamics of MTs, we imaged wild-type and *alp14*Δ cells carrying a GFP-tubulin construct driven by the SV40 promoter (Bratman and Chang, 2007; Snaith *et al.*, 2010) using time-lapse spinning disk confocal microscopy. The number of MT bundles was reduced roughly twofold in *alp14*Δ cells (one to two MT bundles per cell) compared with wild-type cells (three to five bundles per cell; Figure 2B; Tran *et al.*, 2001). MTs were abnormally short on average and exhibited premature catastrophes before reaching the cell tips. The dynamics of MTs were analyzed using kymographs to measure changes in MT length relative to speckle-like fiduciary marks in the MT lattice (Figure 2C; Tran *et al.*, 2001; Janson *et al.*, 2007). This analysis revealed an average twofold decrease in MT assembly rates in *alp14*Δ cells relative to wild-type cells (Figure 2D). MT assembly rates were confirmed by using Mal3-GFP as a marker for growing MT plus ends (Figure 2F). We also found a twofold decrease in MT disassembly rates in *alp14*Δ cells. MTs spent about half as much time in a state of assembly, without a change in the time in disassembly, as compared to wild-type MTs. Of note, MTs spent a significant amount of time in a paused state, which we defined as rate of MT length change <0.5 μm/min (Figure 2E); MTs spent 47% of time in pausing but not at cell tips and an additional 20% of time in pausing at cell tips. This pause phenotype is similar to effects seen with knockdown of the *Drosophila* orthologue Msps (Brittle and Ohkura, 2005;

Currie *et al.*, 2011). Close examination of the kymographs showed that MT assembly profiles were sometimes jagged, suggestive of short periods of MT assembly punctuated by frequent pauses or catastrophe-rescue transitions (Figure 2C). This may be similar to nanoscale excursions seen with MT ends in vitro (Schek *et al.*, 2007; Gardner *et al.*, 2011). Thus these analyses show that *alp14*Δ mutants have a significant defect in persistent, rapid MT assembly.

We tested whether Alp14 affects MT dynamics through effects on the localization of other +TIPS. Some other +TIP mutants, such as *mal3*Δ (EB1), *tip1*Δ (CLIP-170), or *tea2*Δ (kinesin) mutants, also exhibit short MTs (Beinhauer *et al.*, 1997; Browning *et al.*, 2000; Brunner and Nurse, 2000). We found, however, that Mal3, Tip1, and Tea1 still localize properly to the growing MT plus ends in *alp14*Δ mutants (Supplemental Figure S1, C–E). Thus the MT plus end localization of Alp14 and these other +TIPs are independent of each other.

Estimating Alp14 concentration and number of molecules at MT plus ends

We sought to measure the concentration of Alp14 molecules in the cell. We derived estimates by comparing the fluorescence intensity of cells expressing Alp14-GFP to cells expressing GFP fusion proteins that had been counted previously (Wu and Pollard, 2005; Joglekar *et al.*, 2008; Coffman *et al.*, 2011). We found that Alp14-GFP in wild-type cells, which is expressed from its endogenous promoter as the only Alp14 in the cell, is ~0.6 μM (~10,000 molecules/cell), as it has a similar concentration as the myosin II regulatory light chain (Rlc1, estimated at 9600 molecules/cell; Wu and Pollard, 2005; Supplemental Figure S2A). We regard these estimates with caution, especially as they depend on the accuracy of the standards used. Total tubulin dimer concentration in *S. pombe* has been estimated to be 3–5 μM, with roughly one-third polymerized, based on quantitative fluorescence imaging and biochemical approaches (P. Tran, personal communication). Thus these initial estimates indicate that the concentration of Alp14 dimer (see later discussion) is ~10% of tubulin concentration in wild-type cells.

We counted the number of Alp14 molecules on each growing MT plus end by quantitating the fluorescence of individual MT-associated dots. We restricted our analysis to well-isolated, motile Alp14-GFP dots near cell tips. We assumed that the large majority of these motile dots represent Alp14-GFP on individual MT plus ends and not, for instance, many plus ends bundled together (Hoog *et al.*, 2007). By comparing the fluorescence intensities of Alp14 with those of some endocytic patch protein fusions (Basu and Chang, 2011; Sirotkin *et al.*, 2011), we estimated that MT plus end contains on average 70–120 molecules of Alp14-GFP, depending on which standard proteins are used for comparison (Supplemental Figure S2B). In particular, Alp14-GFP dots were slightly brighter than Bzz1-GFP patches, which have been estimated to be on average 75 molecules per patch (Sirotkin *et al.*, 2011), giving an estimate of 96 ± 36 molecules of Alp14 per MT plus end. If we assume that 13 or fewer Alp14 molecules are functioning as active MT polymerases at growing protofilaments, these estimates suggest that the large majority of Alp14 molecules are in the cytoplasm, and of those on the MT plus ends, perhaps only a small subset is actively participating as polymerases at the growing protofilament ends.

Alp14 stimulates MT assembly in vitro

Next we examined the molecular activities of Alp14 in vitro. We purified recombinant full-length Alp14 by using baculovirus expression in insect cells. Recombinant Alp14 is a single species on size exclusion chromatography with a large apparent molecular weight. The large apparent molecular weight of Alp14 suggests that it has an elongated conformation (Figure 5 and Supplemental Figure S3). Alp14 formed stable complexes with soluble tubulin dimer, with a 2:1 binding stoichiometry, similar to *Saccharomyces cerevisiae* Stu2 protein (Al-Bassam *et al.*, 2006). Using sedimentation equilibrium analytical ultracentrifugation, we showed that Alp14 is a homodimer and that Alp14–tubulin complexes contain a single tubulin dimer per Alp14 dimer, as measured by mass differences between Alp14–tubulin complex and Alp14 protein (Supplemental Figure S3).

We analyzed Alp14 activity on dynamic MTs using an assay based upon total internal reflection fluorescence (TIRF) microscopy (Figure 3; Brouhard *et al.*, 2008; Al-Bassam *et al.*, 2010). Biotin- and Texas red–labeled, GMPCPP-stabilized MT seeds were attached onto freshly silanized glass surface via anti-biotin antibodies. Dynamic MTs were polymerized from the MT seeds in the presence of 6 μM tubulin dimer (5.4 μM tubulin plus 0.6 μM Alexa 488–labeled tubulin). This relatively low concentration of tubulin in our TIRF assays is near its physiological concentration in fission yeast (P. Tran, personal communication). Using TIRF microscopy, we imaged the dynamics of individual MTs grown from MT seeds. Parameters of MT dynamics (assembly and disassembly rates, maximal MT length, and catastrophe frequency) were measured in 40–110 individual MTs at each Alp14 concentration, and average values for each parameter were determined by fitting Gaussian distributions to raw data histograms (Supplemental Table S1 and Supplemental Figure S4).

Moderate concentrations of recombinant Alp14 accelerated MT assembly rates to a maximal of threefold, from 0.45 to 1.2 μm/min at 100 nM Alp14 (Figure 3, Supplemental Table S2, and Supplemental Figure S4). Maximal MT length also increased to a maximal of twofold at 100 nM Alp14. However, at this concentration range, Alp14 did not affect MT catastrophe frequency or promote MT rescues. The average MT assembly periods did not increase with the addition of Alp14. Increasing Alp14 concentration to 100 nM accelerated MT disassembly rate by ~30%, from 35 to 45 μm/min. The average MT disassembly period increased up to twofold with increasing Alp14 concentration, most likely because MTs are generally longer.

At higher concentrations (200–1000 nM), rather than accelerate MT assembly rates further, Alp14 promoted MT assembly less effectively (Figure 3, Supplemental Table S1, and Supplemental Figure S4). Dynamic MTs were extremely short and grew very slowly. Assembly rates were similar to or slightly slower than those observed in assays with tubulin alone. In other conditions, high concentrations of Alp14 completely inhibited MT assembly (Figure 3H; see *Materials and Methods*).

We considered whether the inhibitory effects of Alp14 at high concentrations are caused by free Alp14 sequestering tubulin dimers. To test this, we asked whether adding higher concentrations of tubulin would ameliorate these inhibitory effects. As expected, MT assembly rates were higher at 8 and 10 μM tubulin as compared with 6 μM (Walker *et al.*, 1988). At 200 nM, Alp14 increased MT assembly rates by roughly twofold at each tubulin concentration (Figure 3H and Supplemental Table S2). However, higher Alp14 concentrations (250–500 nM) inhibited MT assembly at these tubulin concentrations, although the inhibitory effects were somewhat blunted at higher tubulin concentrations. We then used these data to calculate tubulin dimer association rates (Brouhard *et al.*, 2008). In the absence of Alp14 the tubulin dimer association rate was 4.0 μM/min (Figure 3I), similar to what was previously reported (Brouhard *et al.*, 2008). At 200 nM Alp14, the association rate increased to 6.4 μM/min, whereas at 300 nM Alp14, tubulin association rate was less efficient (4.8 μM/min) and similar to that in the absence of Alp14 (Figure 3I). The effects of Alp14 and tubulin concentration on MT assembly did not correlate in a stoichiometric

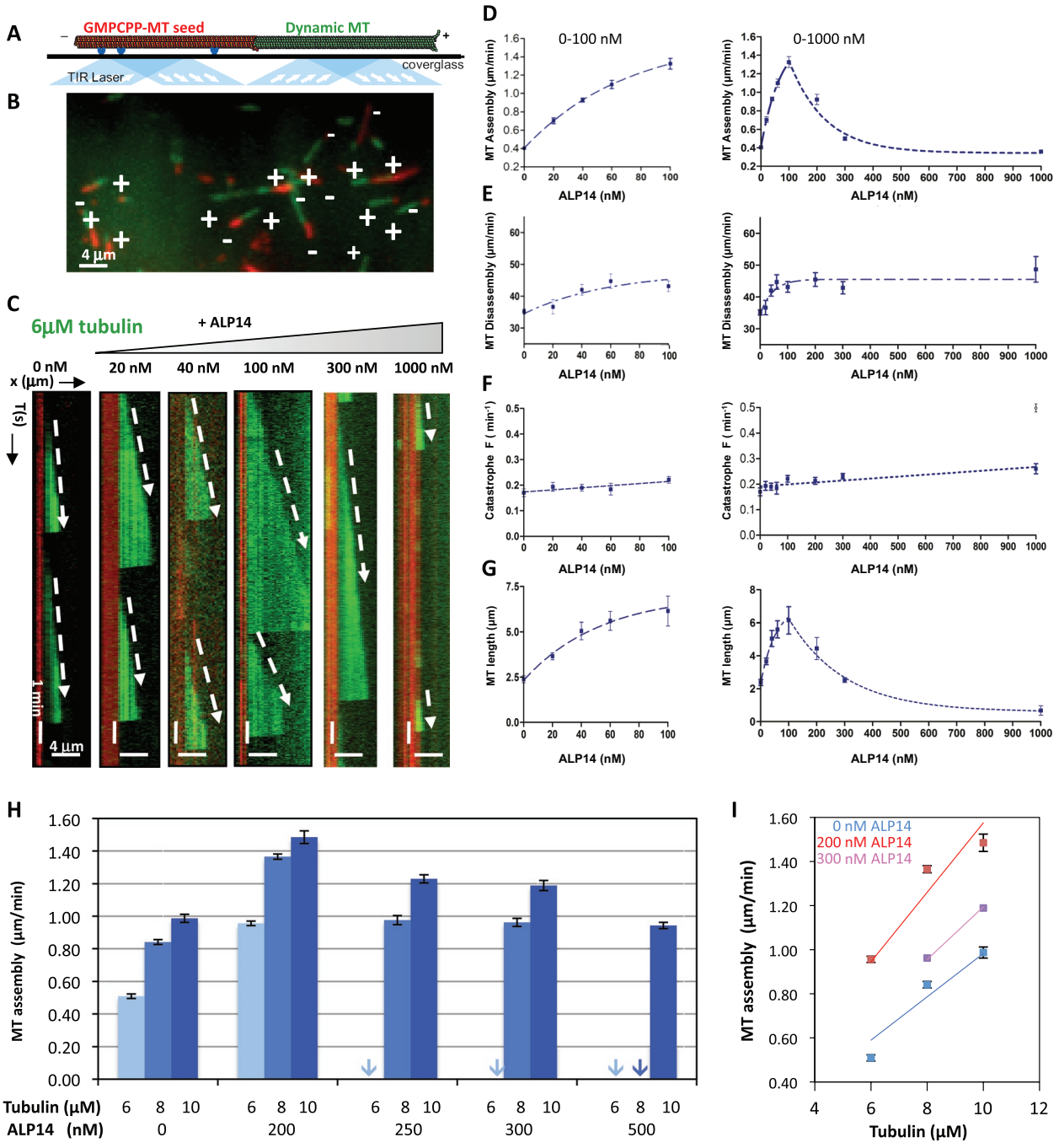

FIGURE 3: Alp14 is moderate MT polymerase at low concentrations in vitro. (A) Scheme for TIRF microscopy assay used to study MT dynamics. Surface-attached anti-biotin antibodies (blue) specifically bind biotin-labeled, GMPCPP-stabilized MT seeds (red). The MT seeds near the surface nucleate Alexa Fluor 488–labeled (green) dynamic MT from 6 µM soluble tubulin dimers in the presence of GTP. TIRF illumination by 564- and 488-nm lasers. Image adapted from Al-Bassam *et al.* (2010). (B) TIRF image of growing MTs. Seeds (red) initiate the assembly of dynamic MTs (green) only at their plus ends (+). In any of the experiments, no assembly occurred at the minus ends (–) in the presence of 6 µM tubulin dimer concentration. (C) Kymographs showing the assembly and disassembly of single dynamic MTs. At 6 µM tubulin, dynamic MTs show slow assembly, rapid disassembly, and frequent catastrophes. At 20–100 nM Alp14, MT assembly rate is incrementally increased, as seen in the slopes of dynamic MT kymographs (broken arrows). The MT assembly rate (at 300–1000 nM) becomes slower, indicating that Alp14 promotes inefficient MT polymerase at the higher concentrations. (D) Effect of Alp14 on the dynamic MT assembly rate. Right, Alp14 accelerates MT assembly by threefold at low (0–100 nM) concentration. At higher concentrations, MT assembly is dramatically decreased. Each point (see also Supplemental Table 1) represents the mean of a Gaussian fit to a distribution of a large number of assembly events measured for each Alp14 concentration (distributions shown in Supplemental Figure S4). (E) Increasing Alp14 concentration causes a moderate increase in MT disassembly rates (Supplemental Table 1). Right, Alp14 increases MT disassembly rate moderately by 25% at the low concentration. Each point (Supplemental Table 1) represents an average Gaussian

manner. For instance, increasing tubulin concentration by 2 μM did not suppress inhibitory effects of increasing Alp14p by 50 nM (a 40-fold difference). Thus these data are not consistent with a simple Alp14 tubulin-sequestering mechanism and suggest that more complex mechanism(s)—for instance, effects at the MT plus end—might underlie these inhibitory effects.

Alp14 tracks growing MT plus ends in vitro

Next we imaged the localization of fluorescent Alp14 molecules in vitro. We purified recombinant Alp14 fused to a C-terminal eGFP (Alp14-GFP) from insect cells using baculovirus expression. We added 25 nM purified recombinant Alp14-GFP to dynamic MTs grown from 6 μM tubulin in which the seed and dynamic portion of MTs were labeled with different concentrations of Texas red–labeled tubulin, leading to intensely labeled MT seeds and weakly labeled dynamic MTs (Figure 4). We observed Alp14-GFP tracking many of the growing MT plus ends. The intensity of Alp14-GFP signal, however, varied among different growing MTs even in the same field. We observed Alp14-GFP dots suddenly appearing at a MT plus end, suggesting that Alp14 binding to MT plus ends may be cooperative. Alp14-GFP molecules also associated with the MT lattice at a lower level and formed dim particles that moved along the lattice in diffusive-type movement; we observed Alp14-GFP particles on the lattice apparently merging with the more intense Alp14 dots at MT plus ends (Figure 4, C, arrow, and D, arrowheads). During catastrophe events, in contrast to Mal3 (EB1), which disappears from the plus end well before MT shrinkage (Busch and Brunner, 2004; Maurer *et al.*, 2012), Alp14 remained associated with MT plus ends until MT shortening ensued and then disappeared from shrinking plus ends (Figure 4, C and D).

The variability in Alp14-GFP binding allowed us to test whether Alp14 promotes MT assembly locally. The total distribution of all dynamic MT assembly events with Alp14-GFP had a very similar distribution to the MT assembly rate observed with 20 nM untagged Alp14. However, MTs plus ends with Alp14-GFP signal at plus ends grew at roughly twofold-higher MT assembly rate than MT plus end without Alp14-GFP throughout their assembly period (Figure 4B). There was no effect on other MT dynamic parameters observed (Figure 4E, Supplemental Figure S5, and Supplemental Table S1). These data show that the localization of Alp14-GFP molecules promotes MT plus end assembly locally.

Alp14 activity requires TOG domain–tubulin binding

Alp14 has two conserved N-terminal TOG domains, TOG1 and TOG2. To test the function of these TOG domains, we characterized an *alp14* mutant protein (Alp14-TOG1,2) in which TOG1 and TOG2 tubulin-binding sites were inactivated by mutating conserved residues at predicted TOG–tubulin-binding interface loops (W23A, R109A in TOG 1 domain; W300A, K381A in TOG2 domain; Al-Bassam *et al.*, 2007). Size exclusion chromatography showed that recombinant Alp14-TOG1,2 had a similar apparent molecular weight as wild-type Alp14, but it did not bind tubulin dimer and did not shift the tubulin into a higher–molecular weight complex (Figure 5A). In vitro, the addition of Alp14-TOG1,2 (20-100 nM) did not accelerate MT assembly rate or increase the average MT length distribution (Figure 5B). Increasing Alp14-TOG1,2 concentration did not increase MT disassembly rate. These results suggest the Alp14 MT polymerase activity requires TOG–tubulin dimer binding.

We next examined the function of the Alp14 TOG domains in vivo. We expressed fragments or full-length *alp14* mutants as mCherry fusions in an *alp14*Δ background and assayed for their ability to rescue the *alp14*Δ phenotype by time-lapse imaging of GFP-labeled MTs (Figure 6). Because the effects of these *alp14* constructs might be highly dosage dependent, we assayed for rescue in a broad range of expression levels and induction times (see later discussion). Expression of a wild-type *alp14*$^+$ gene rescued the MT phenotype of *alp14*Δ mutants, as determined by the appearance of a wild type–like interphase MT cytoskeleton. Cells with mCherry-Alp14 exhibited significantly more MT bundles/cell than a vector control. The mCherry-Alp14 construct localized to MT plus ends as well as the MT lattice; the lattice staining of this construct was more apparent than in the GFP fusion, possibly because of slight differences in expression levels. An N-terminal Alp14 fragment (Alp14$^{1\text{-}509}$; TOG domains only) did not rescue and localized only diffusely in the cytoplasm. A C-terminal Alp14 fragment (Alp14$^{510\text{-}809}$; deletion of TOG domains) did not rescue either but localized to the MT lattice. No specific MT plus end accumulation was seen with the C-terminal Alp14 fragment, although it was difficult to rule out that some portion of these proteins localized to the plus ends in addition to the MT lattice. Alp14-TOG2 and Alp14-TOG12 mutants showed no rescue, whereas the Alp14-TOG1 mutant showed a partial but significant rescue. The Alp14-TOG1 and TOG2 mutants localized to MT plus ends and lattice, whereas the double Alp14-TOG1,2 mutant exhibited only weak MT lattice localization. These data indicate that the TOG domains are necessary but not sufficient to provide Alp14 function and MT plus end localization and that the Alp14 C-terminus is necessary and sufficient for MT lattice association.

distribution fit of a large number of events for different Alp14 concentrations (Supplemental Figure S4). (F) Increasing Alp14 concentration does not affect MT catastrophe frequency (Supplemental Table 1). At 1000 nM two catastrophe frequencies are observed. Each point (Supplemental Table 1) represents an average from a Gaussian fit to the number of catastrophes measured in separate kymographs for each Alp14 concentration (Supplemental Figure S4). (G) Increasing Alp14 concentration increases the MT dynamic length (Supplemental Table 1). Right, Alp14 increases the dynamic length by twofold at low (0–100 nM) concentration. However at the higher concentrations, Alp14 loses polymerase activity. Each point (Supplemental Table 1) represents the mean of a Gaussian fit to a distribution of a large number of assembly events measured for each Alp14 concentration (distributions shown in Supplemental Figure S4). (H) The effect of different Alp14 concentrations on MT assembly rates at 6 (cyan), 8 (blue), and 10 μM (deep blue) tubulin. In the absence of Alp14, MT assembly increased with tubulin concentration. Alp14, 200 nM, induced a twofold increase in MT assembly rate. At higher Alp14 concentrations, Alp14 inhibited MT assembly completely or decreased MT assembly efficiency. Increasing Alp14 concentration (250–500 nM) progressively decreased MT assembly rate to values lower than in the absence of Alp14. See also Supplemental Table S2. (I) The tubulin association rate calculated from the effect of tubulin concentration on MT assembly rate in the absence of Alp14 (blue), 200 nM Alp14 (red), and 300 nM Alp14 (purple). The tubulin association rate was calculated as described (Brouhard *et al.*, 2008). Alp14, 200 nM, increased the association rate from 4.0 (blue) to 6.4 μM/min (red), whereas at 300 nM Alp14 the association rate was decreased to 4.8 μM/min (purple).

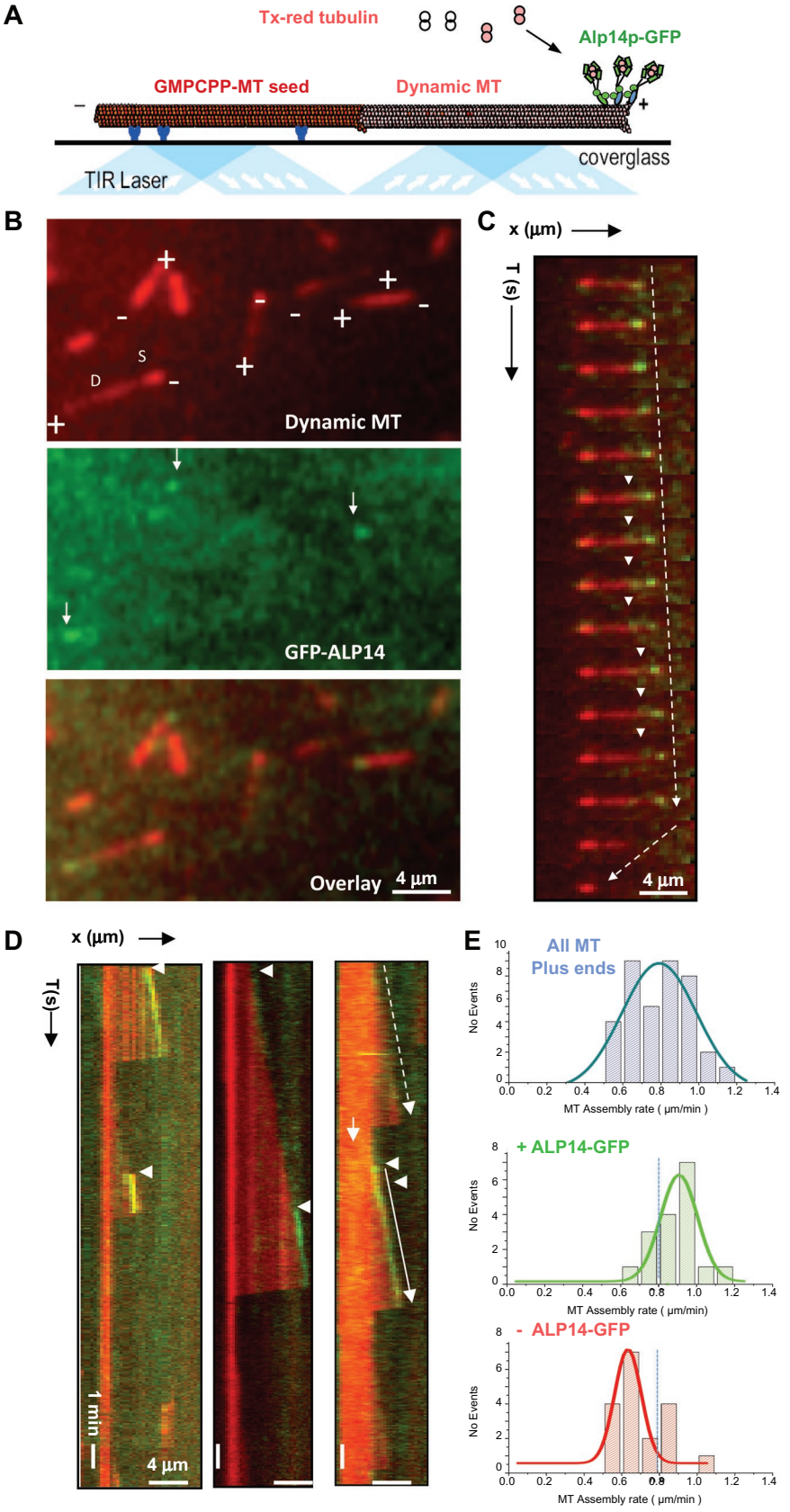

FIGURE 4: Alp14-GFP tracks growing MT plus ends in vitro. (A) Schematic of the TIRF microscopy assay used for imaging MT dynamics and for simultaneous imaging of dynamic MTs and Alp14-GFP localization. Anti-biotin antibodies (blue) bind biotin- and Texas red–labeled, GMPCPP-polymerized MT seeds (red) near the silanized glass surface. The densely labeled Texas red MT seeds nucleate dynamic MT assembly from 6 µM tubulin dimers, less densely labeled with Texas red, in the presence of GTP and 25 nM Alp14-GFP (see *Materials and Methods*). Image adapted from Al-Bassam *et al.* (2010). (B) Raw TIRF image of dynamic MTs and Alp14-GFP. Top, dynamic MTs growing at plus ends of MT seeds. Note that MT seeds have a high fluorescence intensity compared with the dynamic portion of the MTs, which are less intensely labeled with Texas red. Middle, Alp14-GFP. Bottom, overlay showing Alp14-GFP at MT plus ends; note that only some MTs display plus end localization. (C) Montage of Alp14-GFP tracking a growing MT plus end. In successive (10 s/frame), the MT plus end assembles while Alp14-GFP molecules track MT plus ends (broken arrow). Weaker GFP signals attributed to single Alp14-GFP molecules (white arrowheads) diffuse along MT lattices and may accumulate at the plus end. Plus end–tracking Alp14-GFP dissociates and disappears upon MT catastrophe and disassembly (white broken arrow). (D) Kymographs of Alp14-tracking dynamic MT plus ends. Left kymograph, Alp14 tracks a growing MT plus end and then dissociates upon activation of MT catastrophe. As MT plus end assembly reinitiates, Alp14 signal reappears midway through the MT assembly event, and then disappears with MT catastrophe. Middle, MT growing with faint Alp14 signal at the growing MT plus end (top, arrowhead), which then suddenly becomes more intense (lower, arrowhead) and disappears upon the occurrence of MT catastrophes. Right kymograph, three successive MT assembly events from a single MT seed. In the first and third MT assembly events, little or no Alp14-GFP tracking localization is observed at MT plus ends (broken arrow). The second event shows MT plus ends with strong Alp14-GFP localization (white arrowheads). Note that Alp14-GFP molecules bind along the MT seed and diffuse along the lattice over time (arrowhead). (E) Twofold acceleration in MT assembly rate correlates with Alp14-GFP tracking along plus end MTs. Top, Histogram and a Gaussian fit (blue) of all MT assembly events observed with 25 nM Alp14-GFP, showing an intermediate, half-maximal MT assembly rate similar to the distribution observed at 20 nM Alp14 (Supplemental Figure S5). Middle, histogram distribution (green bars) and Gaussian fitting (green line) of Alp14-GFP tracking MT assembly events have a high MT assembly rate. Bottom, histogram distribution (red bars) and Gaussian fitting (red line) of MT assembly events without Alp14 tracking shows lower MT assembly rates. The full MT dynamic parameters for each sets of events are shown in Supplemental Figure S5.

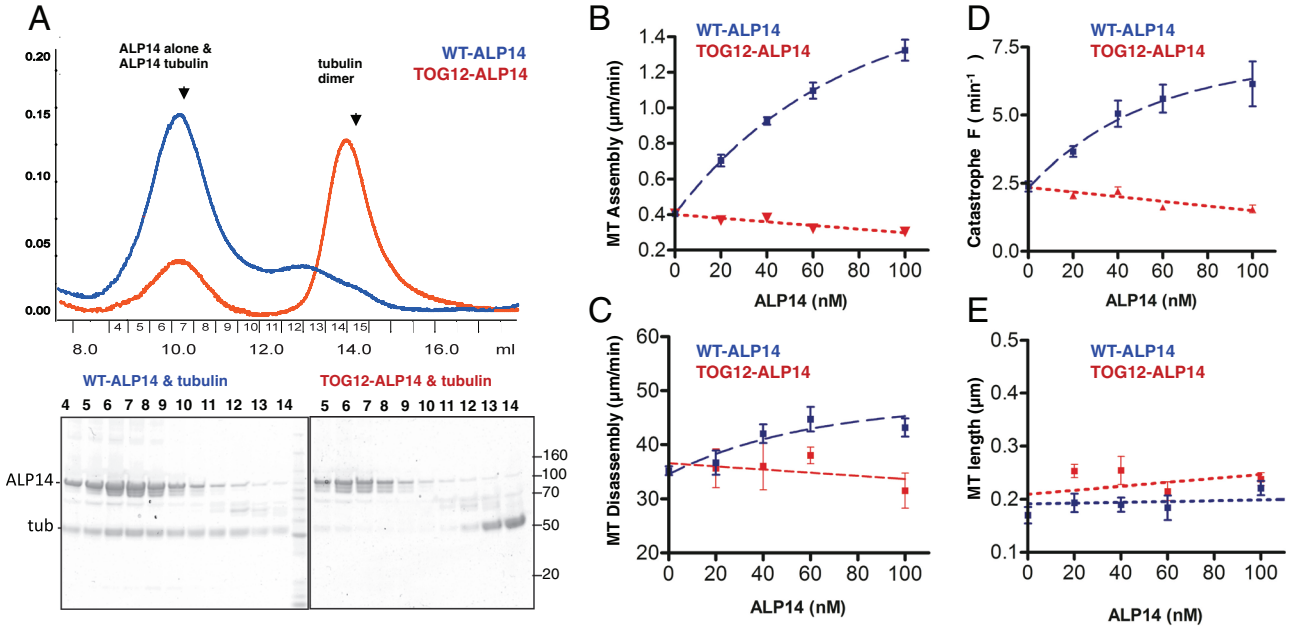

FIGURE 5: An Alp14 TOG-domain mutant is defective in tubulin binding and MT polymerase activity in vitro. (A) Tubulin binding. Wild-type Alp14 or TOG12-Alp14 proteins were mixed with soluble tubulin and assayed for complex formation using size exclusion chromatography. Bottom right, SDS–PAGE of the fractions shows that wild-type Alp14 (blue) and tubulin dimer comigrate in a single peak. TOG12-Alp14 and tubulin dimer migrate as separate peaks, showing that this mutant is defective in tubulin binding (see Supplemental Figure S1). (B–E) Effects of purified TOG1,2 Alp14 on MT dynamics in TIRF in vitro assays (as in Figure 3). Effects of increasing TOG12-Alp14 (red) are shown compared with similar concentrations of wild-type Alp14 (blue; data from Figure 3) on MT assembly (B), MT disassembly (D), MT length (E), and MT catastrophe (F).

Overexpression of Alp14 leads to TOG-dependent loss of microtubules

We noted in these rescue experiments that some *alp14*Δ cells overexpressing Alp14 exhibited an unusual phenotype of complete MT loss. We thus overexpressed a functional mCherry-Alp14 fusion from a thiamine-regulatable *nmt41* promoter on a multicopy plasmid in *alp14+* cells expressing GFP-tubulin. On induction of Alp14 expression, many of the cells lost all GFP-marked MTs (Figure 7A, cell 1). Immunofluorescence staining with anti-tubulin antibody confirmed that these cells, indeed, lacked MTs (Supplemental Figure S6). This complete loss of MTs was notable, as it is a stronger phenotype than treatment with MT-inhibitory drugs (e.g., MBC), which leaves a few stable stubs, or any known null mutants of any single MT-regulatory protein (Tran *et al.*, 2001). Other cells in the population exhibited short MTs or MTs of normal length.

To test whether variability in Alp14 expression levels is responsible for the variable MT phenotypes, we measured the fluorescence intensity of mCherry-Alp14 (or mutant versions of Alp14) in each cell. Cells exhibited highly variable levels (>10-fold variability) of mCherry fluorescence, which is likely to be due to the variable copy number of the plasmids in different cells, as well as variability in protein expression. As a general trend, cells with high levels of Alp14 expression lacked MTs (Figure 7A, cell 1). Intermediate levels were associated with short MTs (Figure 7A, cell 2), and low levels were associated with normal MTs (Figure 7A, cell 3). However, there was some overlap—for instance, between the Alp14 levels giving short or no MTs. Quantitative estimates based on fluorescence intensity measurements of individual cells suggested that, generally, levels of Alp14-mCherry of >2 µM (greater than threefold of wild-type levels) corresponded to a MT-loss phenotype, whereas levels of 1–2 µM (around twofold) corresponded to a short-MT phenotype (Figure 7C).

We tested whether this MT-loss phenotype was dependent on the TOG domains. The MT-loss phenotype was not seen when Alp14 TOG1,2 mutant protein or the C-terminal fragment was overexpressed (Figure 7, B and C). Overexpression of Alp14-TOG1 or Alp14-TOG2 still led to MT loss. Expression of just the TOG domains was equally effective as the full-length Alp14 protein. Expression of the Alp14 C-terminal domain or the Alp14-TOG1,2 mutant produced cells with short MTs similar to that of an *alp14*Δ mutant; it is possible that these proteins confer a dominant-negative effect by dimerizing or competing with the wild-type Alp14 protein. Expression of these constructs in an *alp14*Δ background led to very similar effects. Thus the ability of Alp14 to inhibit MTs is dependent on its ability to bind to tubulin dimers.

We tested the possibility that Alp14 causes MT depolymerization by activating a MT depolymerase, the kinesin-8 heterodimer Klp5/Klp6 (West *et al.*, 2001; Grissom *et al.*, 2009). Interactions of XMAP215 orthologues with kinesin-8 as well as the kinesin-13 (MCAK) have been found in other cell types (Tournebize *et al.*, 2000; Cassimeris and Morabito, 2004; Gandhi *et al.*, 2011). In fission yeast, *alp14*Δ is synthetically lethal with *klp5*Δ or *klp6*Δ (Garcia *et al.*, 2002). Overexpression of Alp14 in a *klp6*Δ background, in which the klp5/6 heterodimer is inactive, still led to MT loss (Supplemental Figure S7). Thus the inhibitory effect of Alp14 is not dependent on Klp5/Klp6 kinesin-8.

These data suggest that as in vitro, Alp14 overexpression also causes MT inhibitory effects in vivo. Our in vivo results are consistent with a tubulin sequestration mechanism, as the overexpression of Alp14 to 2 µM would bind ~25% of the total tubulin in the cell (assuming total tubulin concentration is 4 µM). However, it is possible that more complex mechanism(s) also contribute, as suggested by our in vitro data.

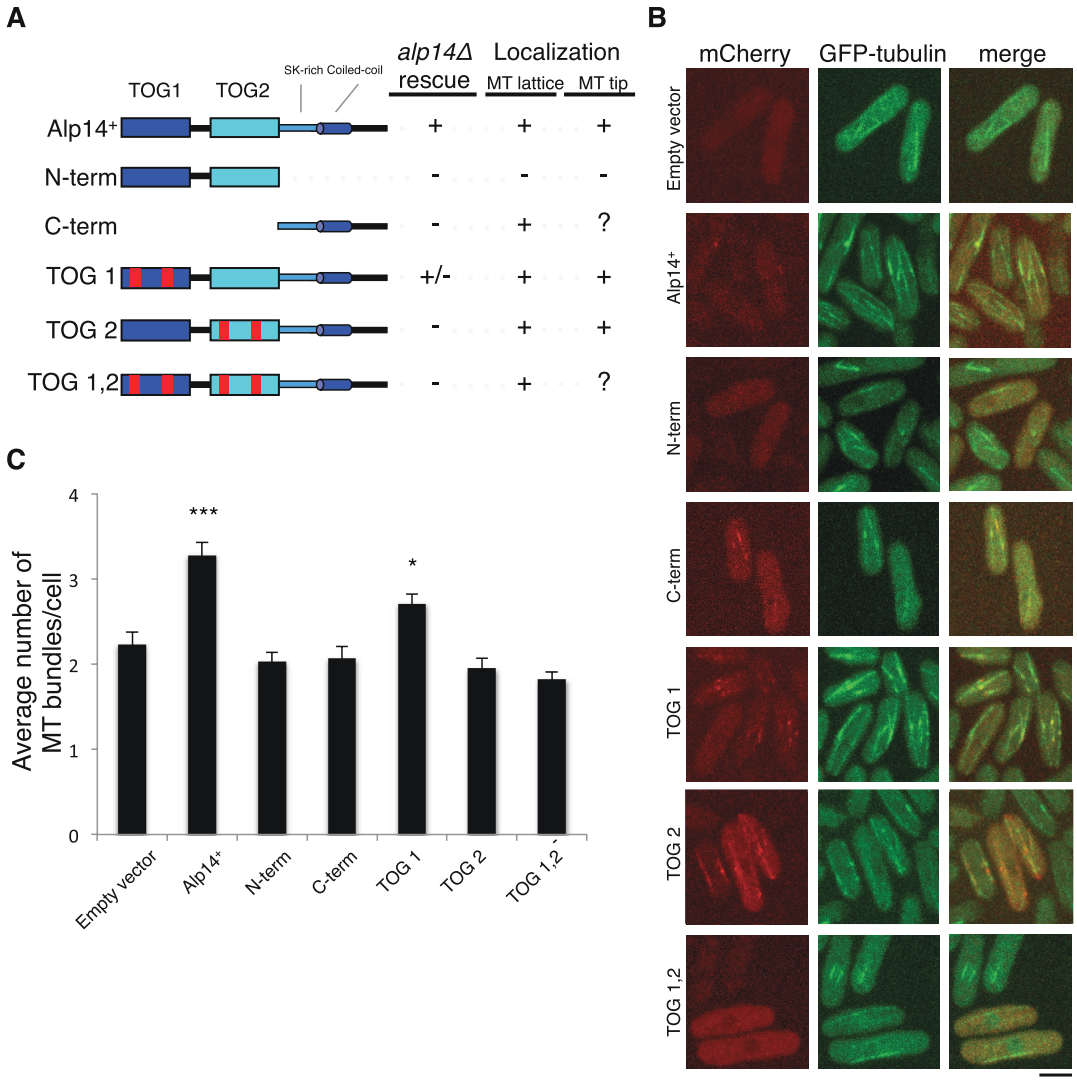

FIGURE 6: Effect of Alp14 domains on *alp14* complementation and localization in vivo. (A) mCherry-Alp4 fusion constructs were expressed from an *nmt42* promoter (medium strength) on multicopy plasmids in *alp14*Δ GFP-tubulin fission yeast cells (FC2484-FC2489). Cells were shifted to inducing conditions (media without thiamine) and examined by time-lapse imaging at multiple time points from 16 to 24 h. Cells with low but detectable level of mCherry proteins were assayed. Table shows a summary of results. Red bars show location of point mutations in the TOG domains. Mutations are: W23A, R109A in TOG1; W300A, K381A in TOG2; Alp14 1-509 in N-term; Alp14 510-809 in C-term. (B) Images of representative fields of *alp14*Δ cells expressing the indicated construct. mCherry images show protein localization to MT lattice, MT plus ends, and/or cytoplasm. MT images show phenotypes in which interphase cells with an *alp14*Δ-like phenotype (not rescued) have a small number of dim bundles, whereas cells with a wild type–like phenotype (rescued) have robust MT bundles. Scale bar, 5 μm. (C) Numbers of interphase MT bundles/cell were counted as a measure of Alp14 rescue by these Alp14 constructs ($n > 30$). These were consistent with other indications of Alp14 activity, including fluorescence intensity of GFP-tubulin in MT bundles and MT dynamics. * $p < 0.01$, *** $p < 0.0001$ on *t*-test compared to empty vector.

DISCUSSION

Alp14 is a conserved MT polymerase

We show here that *S. pombe* Alp14 is a MT polymerase that localizes to the MT plus end and accelerates MT assembly rate two to threefold. In vivo, Alp14 localizes to growing plus ends of interphase MTs, and *alp14* null mutants exhibit abnormally short interphase MTs with twofold decreased assembly and disassembly rates and increased frequency of pausing. We reconstituted activities of Alp14 on dynamic MTs in vitro: purified Alp14 molecules track growing MT plus ends, increase their assembly rate by about threefold, and increase MT disassembly rate slightly (by 30%), without affecting catastrophe or rescue frequencies. These general properties are consistent with those reported for some other XMAP215/Dis1 family members, such as XMAP215 (Gard *et al.*, 2004; Brouhard *et al.*, 2008). Although some orthologues have been studied in vitro and others in vivo, a strength of this work is that we show that the activities of Alp14 in vitro are generally quantitatively consistent with its effects in vivo. Together, these studies provide strong evidence that Alp14 acts as a MT polymerase that promotes faster MT assembly and inhibits MT pausing in the cell. In addition, our quantitative studies show that Alp14 activities are highly dose dependent and exhibit inhibitory effects at higher concentrations both in vitro

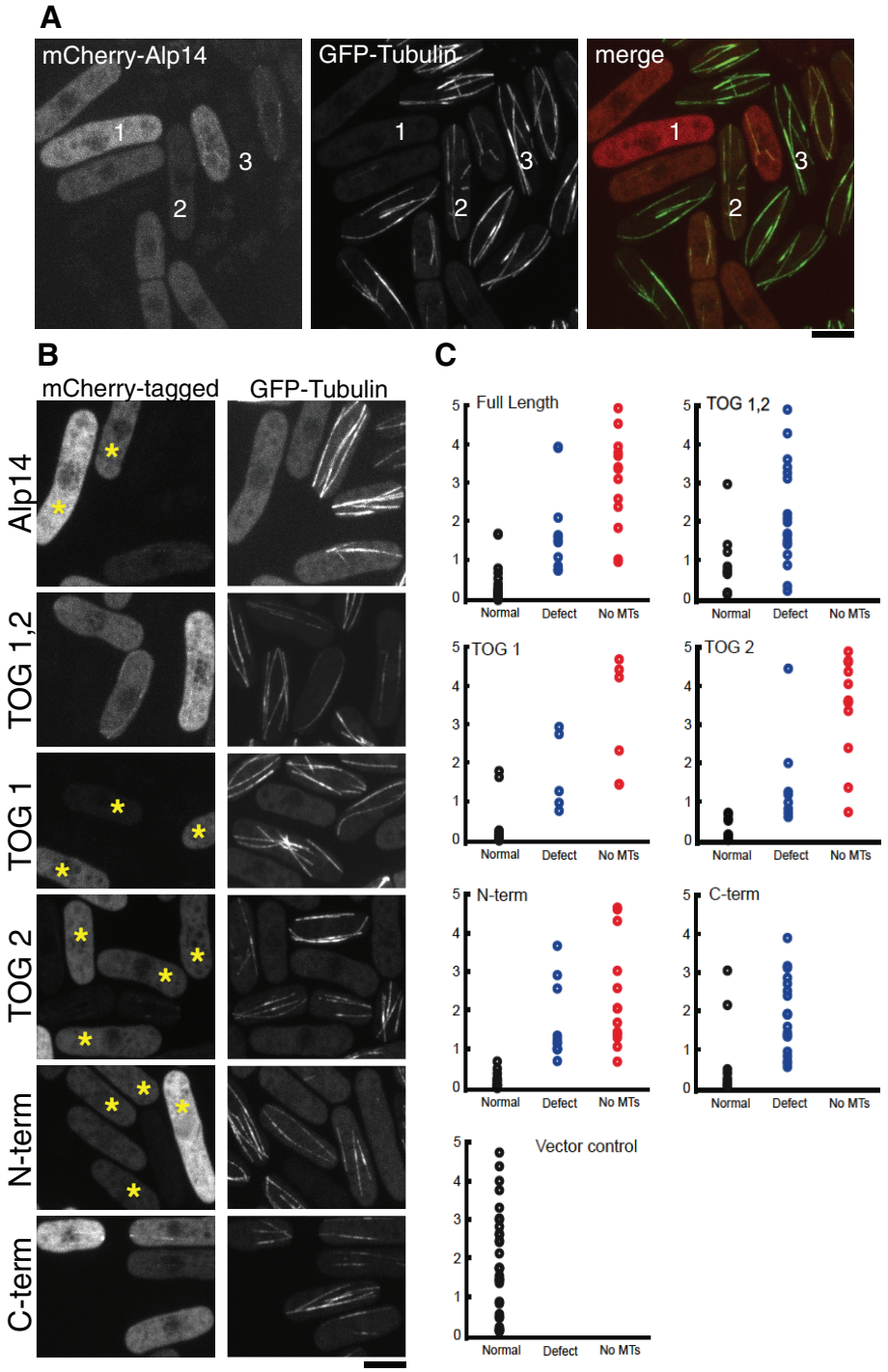

FIGURE 7: Overexpression of Alp14 leads to a TOG-dependent loss of microtubules in vivo. (A) Wild-type GFP-tubulin cells expressing mCherry-Alp14 driven by the thiamine-repressible *nmt42* promoter on multicopy plasmid (FC2477). Image shows a field of fission yeast cells with different levels of Alp14 mCherry expression. Cell expressing high levels lack MTs, those expressing intermediate levels have weakly fluorescing, shorter MTs, and those with no detectable expression have robust MTs. See also Supplemental Figure S6. (B) Images of cells expressing the different mutant constructs (see Figure 6A) in wild-type cells expressing GFP-tubulin (FC2477-2482). Asterisks denote cells lacking MTs. Scale bar, 5 μm. (C) Correlation of Alp14-mCherry expression levels with MT phenotype. Protein concentrations (μM) were estimated by Alp14-mCherry fluorescence intensities over the whole cell. Each dot represents measurement of one cell.

Tracking growing MT plus ends

Alp14 and its orthologues from the XMAP215/Dis1 family define a subclass of MT plus end–tracking proteins distinct from EB-dependent proteins. The majority of known plus end–tracking proteins are believed to be dependent on EB proteins for their localization to growing MT plus ends; EB proteins likely recruit these diverse proteins to the plus end by binding a Ser-X-Gly-Pro sequence (Honnappa *et al.*, 2009; Akhmanova and Steinmetz, 2011). EB proteins have been found to be necessary for the *Drosophila* orthologue Msps for MT plus end localization in vivo (Currie *et al.*, 2011). These in vivo assays are, however, complicated by the fact that depletion of the EB may inhibit Msps localization indirectly by affecting MT dynamics. In contrast, fission yeast Alp14 does not require other +TIP proteins such as Mal3 (EB1) for its plus end localization in vivo, and indeed purified Alp14 molecules track growing plus ends in vitro, as seen also with purified XMAP215 (Brouhard *et al.*, 2008). EB proteins may recognize a conformation of polymerized tubulin regulated by nucleotide binding state (Maurer *et al.*, 2011, 2012). XMAP215 has a much slower residence time at the MT than EB1 proteins in vitro, suggesting that they may use different mechanisms for plus end localization (Bieling *et al.*, 2007; Brouhard *et al.*, 2008). It will be interesting to determine whether XMAP215/Alp14 proteins and EB proteins recognize similar or different structural features of a growing MT plus end. In this study we roughly estimate that ~100 Alp14 molecules are present on the MT plus end, higher than the predicted ≤13 molecules (Brouhard *et al.*, 2008), suggesting that only a small fraction of the Alp14 at plus ends may be actively functioning at any point.

TOG domains and tubulin binding

Our biochemical analysis demonstrates that Alp14 is a homodimer that binds a single tubulin dimer via its TOG domains, much like the budding yeast orthologue Stu2 with which Alp14 shares 20% of its overall sequence identity (Al-Bassam *et al.*, 2006). The binding of tubulin by the TOG domains is critical for Alp14 protein function, as with other TOG-domain proteins (Al-Bassam *et al.*, 2007, 2010; Al-Bassam and Chang, 2011). How TOG domains regulate tubulin dynamics at the MT end, however, remains unclear and controversial (Slep and Vale, 2007; Al-Bassam and Chang, 2011). TOG domains may, for instance, release their bound tubulin dimers into the MT lattice for polymerization; alternatively, the soluble tubulin dimer clutched by multiple TOG domains may not be released but act and in vivo, suggesting that Alp14 has additional, more complex roles in regulating the polymerization state of tubulin (see later discussion).

to transiently stabilize the MT lattice or other tubulin polymerization at the plus end (Brouhard *et al.*, 2008; Al-Bassam and Chang, 2011). In another model TOG domains bind and present tubulin oligomers to a growing MT plus end (Kerssemakers *et al.*, 2006); this, however, is not consistent with the observed saturation stoichiometry of tubulin to XMAP215, Alp14, or Stu2 proteins in solution (Al-Bassam *et al.*, 2006; Brouhard *et al.*, 2008; Widlund *et al.*, 2011). As TOG domains contribute to plus end localization, they may also bind to tubulin in exposed protofilaments at the growing plus end. One possibility is that the two TOG1,2 domains not only clutch a free tubulin dimer, but also bind to an exposed tubulin dimer at the growing lattice to position the Alp14 complex on the growing MT end. Comparison of observations with fission yeast XMAP215 and CLASP orthologues (Alp14 and Cls1) makes it clear that TOG domains from these two families are functionally different; for instance, overexpression of the Cls1 TOG domains hyperstabilizes MTs (Bratman and Chang, 2007), whereas overexpression of Alp14 TOG domains destabilizes MTs in vivo. TOG domains may therefore dictate the different activities of these proteins.

Our mutational analysis of the Alp14 TOG domains begins to reveal functional differences between its two TOG domains. Inactivating mutations in the tubulin-binding loops of the TOG1 domain had only mild effects on MT polymerase activity, whereas mutations in TOG2 domain or in both TOG domains produced a null-like phenotype. In overexpression assays, the single TOG1 and TOG2 mutants still retained ability to depolymerize MTs, whereas the Alp14-TOG1,2 mutant was inactive, suggesting that the single TOG domains can have some activity by themselves. In contrast in Stu2, TOG1 but not TOG2 is sufficient for tubulin binding and is critical for activity in vivo (Al-Bassam *et al.*, 2006). Sequence differences in the tubulin-binding loops in the TOG domains among XMAP215/Dis family members may account for some functional differences between family members (Slep, 2010; Al-Bassam and Chang, 2011).

The C-terminal domain of Alp14 is necessary and sufficient to bind to the MT lattice. In analogy to Stu2, a Ser-Lys–rich (SK-rich) domain in this region following the TOG domains (Alp14 residues 520–673) is likely to be responsible for this lattice-binding activity (Al-Bassam *et al.*, 2006; Al-Bassam and Chang, 2011). Multiple lattice-binding domains have been found in *Drosophila* Msps in some linker regions between TOG domains (Currie *et al.*, 2011). A recent study of the *Xenopus* orthologue XMAP215 shows that a minimal protein consisting of TOG domains and an MT-binding domain from another protein is capable of MT end tracking and polymerase activity, suggesting that the only critical function of this C-terminal domain is in MT lattice binding (Widlund *et al.*, 2011). Alp14 (and orthologues) may initially bind and diffuse on the MT lattice through its C-terminal domain and then accumulate in a cooperative manner at the MT plus end through TOG-dependent interactions with the growing MT plus end (Brouhard *et al.*, 2008).

Dose-dependent inhibitory effects of Alp14

One puzzling aspect of several XMAP215/Dis1 proteins is that under certain conditions, they act as inhibitors of MT formation. In vivo, a threefold increase in Alp14 leads to complete loss of MTs. In vitro, similarly high concentrations of Alp14 cause a decreased MT assembly rate and decreased Alp14 MT polymerase activity. These inhibitory effects are reminiscent of previous findings showing that XMAP215 and Stu2 proteins depolymerize or inhibit MT assembly in vitro when assayed in the absence of soluble tubulin dimer, using nonhydrolyzable GTP analogue, GMPCPP-stabilized MTs (Shirasu-Hiza *et al.*, 2003; van Breugel *et al.*, 2003; Brouhard *et al.*, 2008). Brouhard *et al.* (2008) found that purified XMAP215 associates with shrinking MT plus ends and promotes MT disassembly in the absence of tubulin. However, high concentrations of XMAP215 do not inhibit MT assembly. It has been proposed that in the absence of tubulin, XMAP215 catalyzes MT assembly in reverse, to actively promote disassembly (Brouhard *et al.*, 2008). In this work we observe a strong inhibition of MT assembly when Alp14 concentration is increased. Thus inhibitory effects are seen not only in the absence of soluble tubulin, but also when the ratio of Alp14 to tubulin is high.

One way that Alp14 inhibits MT assembly may be through tubulin sequestration. In vivo, overexpression of Alp14 inhibits MTs at concentrations of ~2 μM, which would be predicted to sequester a significant amount of free tubulin in the cell. This activity is dependent on TOG–tubulin binding activity, and the TOG-domain fragment alone, which does not accumulate on MTs, is sufficient. Genetic analyses suggest that Alp14 does not depolymerize MTs using the Klp5/6 (kinesin-8) depolymerase. Purified Alp14 also has an inhibitory activity in vitro, although at concentrations (>250 μM) well below free tubulin concentrations. We show that simply adding more tubulin does not ameliorate this inhibitory effect, suggesting that more complex inhibitory mechanisms besides tubulin binding and sequestration might be in play. Thus these effects of increasing Alp14 concentration are likely to affect the equilibria of one or more of the multiple steps of Alp14 interacting with the MT. For instance, it is possible that high concentrations cause too many Alp14 molecules to accumulate at the growing MT ends and somehow interfere with MT assembly. The sharp increase in inhibitory activity (from 200 to 250 μM Alp14) is suggestive of a cooperative response. Alp14 could also inhibit MTs by having weak MT depolymerase activity. Consistent with this, we also observe a small twofold decrease in MT disassembly rates in *alp14*Δ cells in vivo and a corresponding but smaller (30%) increase in disassembly rates in vitro. In contrast to XMAP215 and Msps, however, we do not detect Alp14 on the ends of shrinking MTs either in vivo or in vitro.

In conclusion, our studies reveal complex roles of Alp14 in regulating the tubulin dimer–to–MT polymer equilibrium. It might not only promote MT assembly but also contribute to regulation of MT disassembly, as well as binding to a significant pool of free tubulin dimer. The highly dose-dependent effects we observed suggest that Alp14 activity and expression may be carefully regulated in the cell. Further study of Alp14 and how it cycles between its multiple states on and off the MT will provide a framework for understanding novel aspects of MT regulation.

MATERIALS AND METHODS

Yeast strains and growth

S. pombe strains used in this study are listed in Supplemental Table S3. Standard methods for media and genetic manipulation were used (see Pombenet at http://www-bcf.usc.edu/~forsburg/references.html). Deletion strains and strains with integrated tags or promoters were constructed by PCR and homologous recombination. For induction of Alp14 expression from the *nmt42* promoter, cells were first grown in liquid culture in the presence of thiamine and then washed three times and grown for 16–24 h at 30°C in minimal media lacking thiamine. For induction of mRFP-Atb2 (α-tubulin 2; pSB62), cells were prepared as described, but for 22–24 h incubation without thiamine.

Plasmids and oligonucleotides used in this study are listed in Supplemental Tables S4 and S5. For mutagenesis of *alp14*, QuikChange Site-Directed Mutagenesis Kit (Stratagene, Santa Clara, CA) was used. *alp14* wild-type and various mutant constructs were cloned into pREP42X-mCherry backbone plasmid (PSB67) at *Sal*I/*Xho*I and *Xma*I restriction enzyme sites.

Protein expression and purification

Constructs of full-length *S. pombe alp14, alp14-GFP, alp14 TOG,1,2* (residues 1–809) genes were cloned by ligation-independent cloning into a modified baculovirus expression vector, in-frame with an N-terminal histidine (His)–maltose-binding protein tag (MBP) flanked by a TEV protease cleavage site to improve protein expression and solubility. Protein expression was carried out by infecting 2 l of Hi5 insect cells at a density of 1×10^6 cells/ml with the amplified baculoviruses. After 60–72 h, insect cells were harvested and resuspended in lysis buffer (50 mM 4-(2-hydroxyethyl)-1-piperazineethanesulfonic acid [HEPES], 300 mM KCl, 10 mM imidazole, pH 7.0) and lysed with a Dounce homogenizer. Lysates were clarified by centrifugation at 60,000 × *g* for 40 min. His-MBP–tagged fusion proteins were isolated by metal affinity chromatography (NTA-agarose; Qiagen, Valencia, CA) and eluted using a 10–400 mM imidazole linear gradient in lysis buffer. Amylose resin (New England BioLabs, Ipswich, MA) was used to purify the proteins using MBP affinity and was eluted with 20 mM Maltose. The N-terminal His-MBP tags were cleaved overnight with 5 U/ml TEV protease and 1 mM dithiothreitol. Alp14, Alp14-GFP, or TOG12-Alp14 constructs were dialyzed against binding buffer (50 mM HEPES, 100 mM KCl, 5 mM β-mercaptoethanol, pH 7.0), loaded onto a MonoS anion exchange column, and eluted using a gradient of 100–700 mM KCl. Alp14-, Alp14-GFP–, or Alp14-TOG1,2–containing fractions were concentrated and loaded onto a Superdex 200 gel filtration column (16/60) equilibrated with binding buffer containing 400 mM KCl and eluted in 1-ml fractions.

Hydrodynamic and mass analyses

Tubulin dimers were purified from bovine brains using the standard approaches (Mitchison and Kirschner, 1984). For size exclusion chromatography, Alp14 and TOG12-Alp14 constructs were allowed to form complexes with various amounts of tubulin dimer for 5 min and were loaded onto a 10/5 Superdex 200 column preequilibrated at 4°C with 25 mM HEPES, 200 mM KCl, and 1 mM ethylene glycol tetraacetic acid, pH 7.0, and eluted in 0.5 ml fractions. Fractions were evaluated by SDS–PAGE. Apparent molecular masses and Stokes radii of the Alp14 alone and in complex with tubulin dimer were determined by calibrating the size exclusion column with protein standards (Bio-Rad, Hercules, CA). Stokes radii for different samples were calculated as averages of the Porath and Laurent–Killander Stokes radii, which matched closely. For sedimentation equilibrium analytical ultracentrifugation experiments, purified fractions of Alp14 and Alp14-tubulin complexes were loaded in an Optima XLA (Beckman Coulter, Brea, CA) analytical ultracentrifuge as previously described (Al-Bassam *et al.*, 2006).

In vitro microtubule assays

Total internal reflection microscopy studies of Alp14 with dynamic MTs in vitro were based on a modified version of the approach described by Al-Bassam *et al*. (2010). Tubulin dimers were labeled with succinimidyl ester or tetrafluorophenyl esters of biotin, Alexa Fluor 488, or Texas Red esters (Invitrogen, Carlsbad, CA) and recycled as described in Mitchison and Kirschner (1984). MT seeds were polymerized with 2 mM GMPCPP from a 1.8 mg/ml mixture of Texas red–labeled, biotin-labeled, and unlabeled tubulin dimers in a 4:2:1 ratio at 37°C for 2 h. Glass coverslips were cleaned and silanized as described (Brouhard *et al.*, 2008). Flow cells were constructed as previously described (Al-Bassam *et al.*, 2010). Fully sealed flow cells were mounted onto a Nikon TIRF microscope with a 60× Nikon TIRF lens (Nikon, Melville, NY) warmed to 35°C by a temperature collar. MTs were imaged in the evanescent wave by 488- and 568-nm laser excitation. Dual-emission data were collected in 2.1-s intervals for 18.4 min (1125 s) with a side-entry iXon EM charge-coupled device (CCD; Andor, South Windsor, CT) with each channel projected onto split fields. MT assembly experiments in Figure 3, H and I, were performed using porcine instead of the bovine brain tubulin used for the other experiments. Some subtle differences in the degree of MT growth at high Alp14 concentrations (250–1000 nM) may be due to differences in tubulin or Alp14 protein preparations but did not affect our general conclusions.

Image analysis and measurement of MT dynamics

Image stacks were analyzed using the EMBL-ImageJ software (National Institutes of Health, Bethesda, MD). Briefly, raw image stacks were photobleach corrected by normalization of total image intensity to the average intensity of the first image and scaling up the value of bleached images accordingly. Kymographs were used to measure parameters of MT dynamics. Frequencies of MT catastrophe were measured for individual dynamic MTs formed from each MT seed by dividing the number of events with the duration of MT assembly (for catastrophe). Raw distributions for assembly rates, disassembly rates, catastrophe frequency, and rescue frequencies were fit by single or multiple Gaussian functions to determine the average and error values for each parameter using the program Origin (OriginLab, Northampton, MA) and are shown in Supplemental Figures S4 and S5.

For live cell imaging, fission yeast cells were imaged on 2% YE agar pads under a coverslip. Microscopy was performed with a spinning disk confocal microscope system (PerkinElmer, Waltham, MA; Nikon; Solamere, Salt Lake City, UT) with an electron-multiplying CCD camera (Hamamatsu, Hamamatsu, Japan). Images were acquired and analyzed with ImageJ and OpenLab software (Improvision, PerkinElmer). Kymographs were constructed with the Volume Slicing tool in OpenLab. Dynamic parameters were determined largely from kymographs using MT speckled patterns as fiduciary marks to account for movement of the MT bundle. To determine the number of Alp14 molecules in a cell, we compared florescence intensities of cells expressing mCherry-Alp14 with those expressing Rlc1-mCherry or Arc5-mCherry at endogenous levels, as described. Ratios of the intensities of single dots and cell-wide signal were used to estimate the cytoplasmic pool versus particular forms of Alp14 molecules.

ACKNOWLEDGMENTS

We thank Steve Harrison and Antoine van Ojien, in whose laboratories at Harvard Medical School the in vitro work was largely done; T. Toda and P. Tran for materials; P. Tran for communication of unpublished data; and members of the Chang lab, G. Brouhard, J. Howard, and J. Q. Wu, for discussion. This work was supported by National Institutes of Health Grants R00 GMO8429 to J.A.-B. and R01 GM069670 to F.C., National Institutes of Health Training Grant DK07328 to H.K., and Fulbright Postdoctoral Award to I.F.P.

REFERENCES

Akhmanova A, Steinmetz MO (2008). Tracking the ends: a dynamic protein network controls the fate of microtubule tips. Nat Rev Mol Cell Biol 9, 309–322.

Akhmanova A, Steinmetz MO (2011). Microtubule end binding: EBs sense the guanine nucleotide state. Curr Biol 21, R283–R285.

Al-Bassam J, Chang F (2011). Regulation of microtubule dynamics by TOG-domain proteins XMAP215/Dis1 and CLASP. Trends Cell Biol 21, 604–614.

Al-Bassam J, Kim H, Brouhard G, van Oijen A, Harrison SC, Chang F (2010). CLASP promotes microtubule rescue by recruiting tubulin dimers to the microtubule. Dev Cell 19, 245–258.

Al-Bassam J, Larsen NA, Hyman AA, Harrison SC (2007). Crystal structure of a TOG domain: conserved features of XMAP215/Dis1-family TOG domains and implications for tubulin binding. Structure 15, 355–362.

Al-Bassam J, van Breugel M, Harrison SC, Hyman A (2006). Stu2p binds tubulin and undergoes an open-to-closed conformational change. J Cell Biol 172, 1009–1022.

Basu R, Chang F (2011). Characterization of dip1p reveals a switch in Arp2/3-dependent actin assembly for fission yeast endocytosis. Curr Biol 21, 905–916.
Beinhauer JD, Hagan IM, Hegemann JH, Fleig U (1997). Mal3, the fission yeast homologue of the human APC-interacting protein EB-1 is required for microtubule integrity and the maintenance of cell form. J Cell Biol 139, 717–728.
Bieling P, Laan L, Schek H, Munteanu EL, Sandblad L, Dogterom M, Brunner D, Surrey T (2007). Reconstitution of a microtubule plus-end tracking system in vitro. Nature 450, 1100–1105.
Bratman SV, Chang F (2007). Stabilization of overlapping microtubules by fission yeast CLASP. Dev Cell 13, 812–827.
Bratman SV, Chang F (2008). Mechanisms for maintaining microtubule bundles. Trends Cell Biol 18, 580–586.
Brittle AL, Ohkura H (2005). Mini spindles, the XMAP215 homologue, suppresses pausing of interphase microtubules in *Drosophila*. EMBO J 24, 1387–1396.
Brouhard GJ, Stear JH, Noetzel TL, Al-Bassam J, Kinoshita K, Harrison SC, Howard J, Hyman AA (2008). XMAP215 is a processive microtubule polymerase. Cell 132, 79–88.
Browning H, Hayles J, Mata J, Aveline L, Nurse P, McIntosh JR (2000). Tea2p is a kinesin-like protein required to generate polarized growth in fission yeast. J Cell Biol 151, 15–28.
Brunner D, Nurse P (2000). CLIP170-like tip1p spatially organizes microtubular dynamics in fission yeast. Cell 102, 695–704.
Busch KE, Brunner D (2004). The microtubule plus end-tracking proteins mal3p and tip1p cooperate for cell-end targeting of interphase microtubules. Curr Biol 14, 548–559.
Busch KE, Hayles J, Nurse P, Brunner D (2004). Tea2p kinesin is involved in spatial microtubule organization by transporting tip1p on microtubules. Dev Cell 6, 831–843.
Cassimeris L, Morabito J (2004). TOGp, the human homolog of XMAP215/Dis1, is required for centrosome integrity, spindle pole organization, and bipolar spindle assembly. Mol Biol Cell 15, 1580–1590.
Coffman VC, Wu P, Parthun MR, Wu JQ (2011). CENP-A exceeds microtubule attachment sites in centromere clusters of both budding and fission yeast. J Cell Biol 195, 563–572.
Currie JD, Stewman S, Schimizzi G, Slep KC, Ma A, Rogers SL (2011). The microtubule lattice and plus-end association of *Drosophila* Mini spindles is spatially regulated to fine-tune microtubule dynamics. Mol Biol Cell 22, 4343–4361.
Gandhi SR, Gierlinski M, Mino A, Tanaka K, Kitamura E, Clayton L, Tanaka TU (2011). Kinetochore-dependent microtubule rescue ensures their efficient and sustained interactions in early mitosis. Dev Cell 21, 920–933.
Garcia MA, Koonrugsa N, Toda T (2002). Spindle-kinetochore attachment requires the combined action of Kin I-like Klp5/6 and Alp14/Dis1-MAPs in fission yeast. EMBO J 21, 6015–6024.
Garcia MA, Vardy L, Koonrugsa N, Toda T (2001). Fission yeast ch-TOG/XMAP215 homologue Alp14 connects mitotic spindles with the kinetochore and is a component of the Mad2-dependent spindle checkpoint. EMBO J 20, 3389–3401.
Gard DL, Becker BE, Josh Romney S (2004). MAPping the eukaryotic tree of life: structure, function, and evolution of the MAP215/Dis1 family of microtubule-associated proteins. Int Rev Cytol 239, 179–272.
Gard DL, Kirschner MW (1987). A microtubule-associated protein from *Xenopus* eggs that specifically promotes assembly at the plus-end. J Cell Biol 105, 2203–2215.
Gardner MK, Charlebois BD, Janosi IM, Howard J, Hunt AJ, Odde DJ (2011). Rapid microtubule self-assembly kinetics. Cel 146, 582–592.
Grissom PM, Fiedler T, Grishchuk EL, Nicastro D, West RR, McIntosh JR (2009). Kinesin-8 from fission yeast: a heterodimeric, plus-end-directed motor that can couple microtubule depolymerization to cargo movement. Mol Biol Cell 20, 963–972.
Honnappa S *et al.* (2009). An EB1-binding motif acts as a microtubule tip localization signal. Cell 138, 366–376.
Hoog JL, Schwartz C, Noon AT, O'Toole ET, Mastronarde DN, McIntosh JR, Antony C (2007). Organization of interphase microtubules in fission yeast analyzed by electron tomography. Dev Cell 12, 349–361.
Hsu KS, Toda T (2011). Ndc80 internal loop interacts with Dis1/TOG to ensure proper kinetochore-spindle attachment in fission yeast. Curr Biol 21, 214–220.
Janson ME, Loughlin R, Loiodice I, Fu C, Brunner D, Nedelec FJ, Tran PT (2007). Crosslinkers and motors organize dynamic microtubules to form stable bipolar arrays in fission yeast. Cell 128, 357–368.
Joglekar AP, Salmon ED, Bloom KS (2008). Counting kinetochore protein numbers in budding yeast using genetically encoded fluorescent proteins. Methods Cell Biol 85, 127–151.
Kerssemakers JW, Munteanu EL, Laan L, Noetzel TL, Janson ME, Dogterom M (2006). Assembly dynamics of microtubules at molecular resolution. Nature 442, 709–712.
Maurer SP, Bieling P, Cope J, Hoenger A, Surrey T (2011). GTPgammaS microtubules mimic the growing microtubule end structure recognized by end-binding proteins (EBs). Proc Natl Acad Sci USA 108, 3988–3993.
Maurer SP, Fourniol FJ, Bohner G, Moores CA, Surrey T (2012). EBs recognize a nucleotide-dependent structural cap at growing microtubule ends. Cell 149, 371–382.
Mitchison T, Kirschner M (1984). Dynamic instability of microtubule growth. Nature 312, 237–242.
Nabeshima K, Kurooka H, Takeuchi M, Kinoshita K, Nakaseko Y, Yanagida M (1995). p93dis1, which is required for sister chromatid separation, is a novel microtubule and spindle pole body-associating protein phosphorylated at the Cdc2 target sites. Genes Dev 9, 1572–1585.
Nakaseko Y, Goshima G, Morishita J, Yanagida M (2001). M phase-specific kinetochore proteins in fission yeast: microtubule-associating Dis1 and Mtc1 display rapid separation and segregation during anaphase. Curr Biol 11, 537–549.
Roque H, Ward JJ, Murrells L, Brunner D, Antony C (2010). The fission yeast XMAP215 homolog Dis1p is involved in microtubule bundle organization. PLoS One 5, e14201.
Sato M, Toda T (2007). Alp7/TACC is a crucial target in Ran-GTPase-dependent spindle formation in fission yeast. Nature 447, 334–337.
Sato M, Vardy L, Angel Garcia M, Koonrugsa N, Toda T (2004). Interdependency of fission yeast Alp14/TOG and coiled coil protein Alp7 in microtubule localization and bipolar spindle formation. Mol Biol Cell 15, 1609–1622.
Sawin KE, Tran PT (2006). Cytoplasmic microtubule organization in fission yeast. Yeast 23, 1001–1014.
Schek HT 3rd, Gardner MK, Cheng J, Odde DJ, Hunt AJ (2007). Microtubule assembly dynamics at the nanoscale. Curr Biol 17, 1445–1455.
Shirasu-Hiza M, Coughlin P, Mitchison T (2003). Identification of XMAP215 as a microtubule-destabilizing factor in *Xenopus* egg extract by biochemical purification. J Cell Biol 161, 349–358.
Sirotkin V, Berro J, Macmillan K, Zhao L, Pollard TD (2011). Quantitative analysis of the mechanism of endocytic actin patch assembly and disassembly in fission yeast. Mol Biol Cell 21, 2894–2904.
Slep KC (2010). Structural and mechanistic insights into microtubule end-binding proteins. Curr Opin Cell Biol 22, 88–95.
Slep KC, Vale RD (2007). Structural basis of microtubule plus end tracking by XMAP215, CLIP-170, and EB1. Mol Cell 27, 976–991.
Snaith HA, Anders A, Samejima I, Sawin KE (2010). New and old reagents for fluorescent protein tagging of microtubules in fission yeast; experimental and critical evaluation. Methods Cell Biol 97, 147–172.
Tournebize R, Popov A, Kinoshita K, Ashford AJ, Rybina S, Pozniakovsky A, Mayer TU, Walczak CE, Karsenti E, Hyman AA (2000). Control of microtubule dynamics by the antagonistic activities of XMAP215 and XKCM1 in *Xenopus* egg extracts. Nat Cell Biol 2, 13–19.
Tran PT, Marsh L, Doye V, Inoue S, Chang F (2001). A mechanism for nuclear positioning in fission yeast based on microtubule pushing. J Cell Biol 153, 397–411.
van Breugel M, Drechsel D, Hyman A (2003). Stu2p, the budding yeast member of the conserved Dis1/XMAP215 family of microtubule-associated proteins is a plus end-binding microtubule destabilizer. J Cell Biol 161, 359–369.
Walker RA, O'Brien ET, Pryer NK, Soboeiro MF, Voter WA, Erickson HP, Salmon ED (1988). Dynamic instability of individual microtubules analyzed by video light microscopy: rate constants and transition frequencies. J Cell Biol 107, 1437–1448.
West RR, Malmstrom T, Troxell CL, McIntosh JR (2001). Two related kinesins, klp5+ and klp6+, foster microtubule disassembly and are required for meiosis in fission yeast. Mol Biol Cell 12, 3919–3932.
Widlund PO, Stear JH, Pozniakovsky A, Zanic M, Reber S, Brouhard GJ, Hyman AA, Howard J (2011). XMAP215 polymerase activity is built by combining multiple tubulin-binding TOG domains and a basic lattice-binding region. Proc Natl Acad Sci USA 108, 2741–2746.
Wu JQ, Pollard TD (2005). Counting cytokinesis proteins globally and locally in fission yeast. Science 310, 310–314.